Microfluidics and Nanofluidics (2019) 23:91
https://doi.org/10.1007/s10404-019-2257-3

SHORT COMMUNICATION

Drug dosage for microneedle-based transdermal drug delivery systems utilizing evaporation-induced droplet transport

Andreas Tröls[1] · Marcus A. Hintermüller[1] · Mahdi Saeedipour[2] · Stefan Pirker[2] · Bernhard Jakoby[1]

Received: 26 February 2019 / Accepted: 4 June 2019 / Published online: 12 June 2019

Abstract

We present a setup for directed loading of standard microneedle arrays for transdermal drug delivery with the respective therapeutic agent. The necessity to dose medical drugs according to their particular utilization requires an exact volumetric measure of the particular drug, which is usually provided as a liquid. This is achieved by arranging a metallic plate above the array featuring a set of holes aligned with the microneedles underneath. The plate is coated with a superhydrophobic layer. To initiate the filling, droplets are deposited on said holes, where the volume needs to be above the desired load for an individual needle, but the exact dosage is not required. Evaporation of these sessile droplets, after some time, leads to the falling of the droplets through the microfluidic plate, delivering an exact amount of liquid drug to the needles underneath. The proposed setup is easy to implement and parallelize, assisting in the task of accurate and high throughput coating of microneedle-based transdermal drug delivery devices.

Keywords Droplet based microfluidics · Liquid dosage · Superhydrophobic surfaces · Microneedle array

1 Introduction

Transdermal drug delivery systems utilizing microneedle arrays provide a minimally invasive option to deliver drugs in a sustained and at a controlled rate, with the advantage of patient-friendly application and potential for self-administration (Prausnitz and Langer 2008; Lee et al. 2018). The microneedles of few hundred microns height feature distinct advantages compared to traditional means of drug delivery such as oral ingestion and hypodermic injection (Patil 2017). Usually, a lower dosage is required for microneedle patches, compared to oral ingestion, as digestion and first-pass metabolism are circumvented (Lee et al. 2018). Also, hypodermic injection requires penetration into subcutaneous tissue using a needle (usually done by a trained administrator), causing pain and therefore reducing patient's compliance (Alkilani et al. 2015).

Different approaches concerning the design of microneedle arrays have been reported in literature. Most common variants are solid, dissolving and hollow microneedles (Larrañeta et al. 2016). When utilizing solid or dissolving microneedles, the surface of the needles has to be coated with an exact dose of the drug.

In this contribution, we propose an efficient method for precise dosage of homogenous liquids employing a superhydrophobic perforated plate, which can be potentially used for coating of microneedle arrays. Figure 1 shows the principle of operation in combination with solid microneedles. A rough amount of the liquid to dose is placed on the holes of the plate (Fig. 1a). The droplets resting on the holes then gradually evaporate (Fig. 1b), until they are small enough to be dragged through the hole due to gravitational forces and coat the microneedles underneath (Fig. 1c). Then, the needle patch is placed on the skin (Fig. 1d), thereby penetrating the epidermis (Fig. 1e), and leaving behind the drug after removing the needle patch subsequently (Fig. 1f).

Andreas Tröls and Marcus A. Hintermüller contributed equally to this work.

Electronic supplementary material The online version of this article (https://doi.org/10.1007/s10404-019-2257-3) contains supplementary material, which is available to authorized users.

✉ Andreas Tröls
andreas.troels@jku.at

[1] Institute for Microelectronics and Microsensors, Johannes Kepler University Linz, Linz, Austria

[2] Department of Particulate Flow Modelling, Johannes Kepler University Linz, Linz, Austria

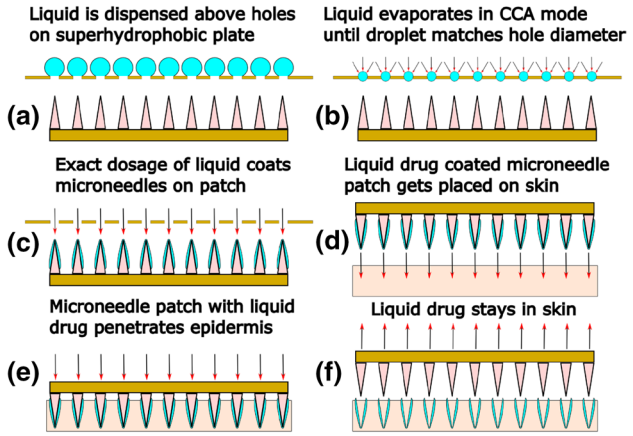

Fig. 1 Schematic use as medical coating system for microneedles

Exact drug dosage using a dip-coating process depends on the particular conditions, of, e.g., exposure time of the needles to the solution, surface tension matching between needle material and liquid, liquid material properties and structure of the needles. If the conditions are not met sufficiently well, the dip-coating process results in patchy coverage of the needles (Gill and Prausnitz 2007). Since dosing with the proposed setup is spatially and temporally separated from the actual coating of the needles, meeting the right conditions is easier.

Other techniques, like the electrohydrodynamic atomization (EHDA) process or ink-jet printing can produce controlled coating thicknesses, but special equipment is required (Haj-Ahmad et al. 2015). Also gas jet- or spray drying methods have been considered (Chen et al. 2011; McGrath et al. 2011). The proposed method is easy to implement and highly parallelizable, potentially enabling small-scale and mass production.

2 Experimental setup

Figure 2 shows the experimental setup of the proposed coating method, featuring three stages of the coating process, compared to Fig. 1a–c. The top stage contains the droplet dispenser, which was fabricated by 3D printing (Stratasys™ Objet 30 Pro), for roughly dispensing droplets of the liquid on the dosing plane by means of a 3×3 dispenser needle array. The top side features small wells for each needle, where the liquid can be placed.

The second stage features the perforated dosage plate, etched from nickel silver (also known as German nickel), with a 3×3 array of holes that was coated with the commercially available impregnation spray NeverWet™. Wet etching of the holes was preferred over drilling, since it avoids drilling specific problems like possible mechanical

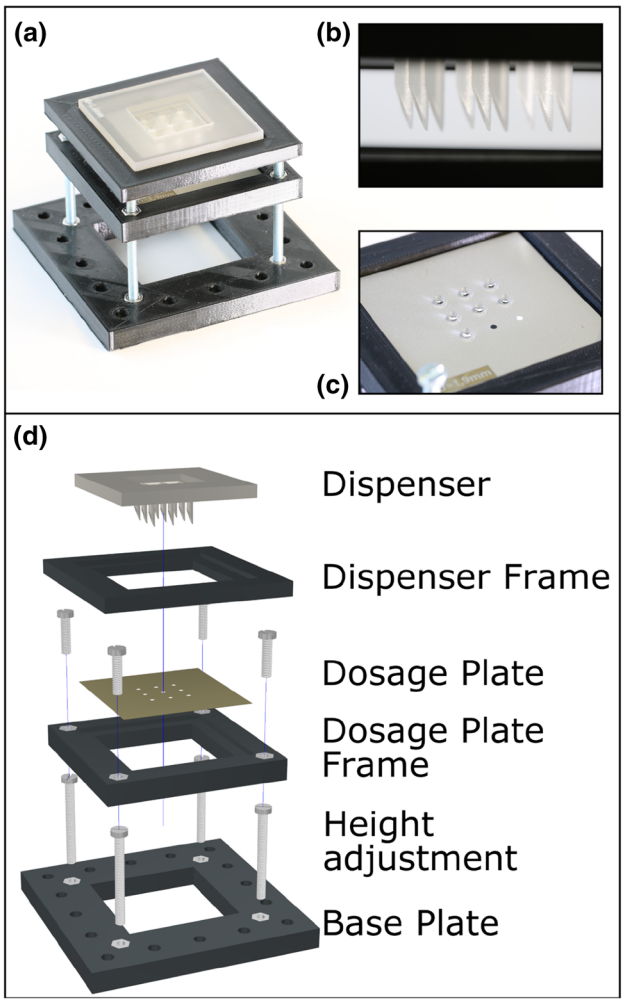

Fig. 2 **a–c** Photograph of the setup. **d** Exploded view schematic of the setup

deformations and burrs around the circumference of the hole. As our application requires an even dosage plate surface, it can be expected that the etched holes are more suitable than drilled ones. After coating, a contact angle between the plane and water of about $\theta_0 = 154°$ has been measured (Tröls et al. 2016), classifying it as superhydrophobic (Wang and Jiang 2007). Due to the structure of this hydrophobic layer, a droplet rests on it in a suspended Cassie–Baxter state on top of the rough plane surface (Marmur 2003). The contact angle hysteresis on these surfaces is relatively small and droplets can easily roll off (Zang et al. 2013).

The superhydrophobic surface is required to ensure that the droplets evaporate in a so-called constant contact angle (CCA) mode, meaning that the contact angle remains constant, while the contact radius decreases during evaporation (Berthier 2013). This is the preferred mode, as the droplets can pass through the hole once the contact radius is small enough. Dash and Garimella pointed out that even

on a hydrophobic surface (e.g., PTFE coating, $\theta_0 \sim 120°$), a droplet evaporates initially in a, for our purposes unwanted, constant contact radius (CCR) mode, due to contact line pinning resulting from contact angle hysteresis (Dash and Garimella 2013). Using a superhydrophobic surface, contact angle hysteresis can be minimized; therefore, no contact line pinning interfering with the evaporation process in a pure CCA mode was observed (Dash and Garimella 2014).

The microneedle array would be placed at the bottom of the third stage (only represented by the base plate in Fig. 2). The dispenser frame, dosage plane frame and base plate were 3D-printed with an Ultimaker™ 3 Extended printer. The height adjustment screws are used to cancel out any tilting of the plane, ensuring perfect balance due to the very low roll-off angle of the droplets. Figure 2a shows the fully assembled device; Fig. 2b, c show detailed images of the dispenser needles and the superhydrophobic perforated microfluidic plate. The dispenser needle array gets positioned exactly above the hole array. Figure 2c shows the water droplets resting on top of the holes. Figure 2d shows an exploded view of all components of the transdermal drug delivery coating system.

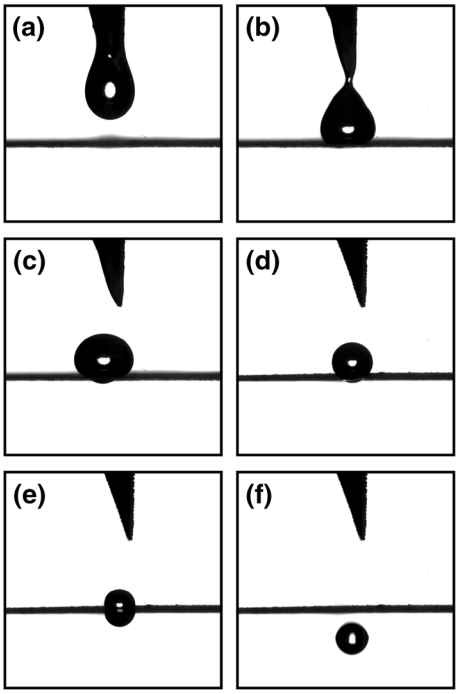

Fig. 3 Sequence of the operational principle. **a**, **b** Fast dispensation on the perforated plate. **c**, **d** Evaporation. **e**, **f** Application with geometry determined dosage of the liquid

3 Results

The dosing process can be broken down into two steps. First, a rough dosage step by the dispenser takes place, followed by an exact dosage step governed by the hole geometry after the liquid evaporates. The whole procedure, from dispensing to droplet release is shown in Fig. 3, recorded with a Photron™ SA4 Fastcam high-speed camera @ 500 fps. In the shown example, the hole diameter was $d = 1.9$ mm. The liquid used in all experiments was deionized (DI) water.

Figure 3a shows a water droplet flowing along the needle-like structure of the dispenser stage. In Fig. 3b, the droplet finally detaches from the tip of the needle and subsequently lands on the hole of the dosage stage. A video of the dispensing process can be found in the supplementary material. Figure 3c, d show the evaporation of the DI water in CCA mode until the droplet's dimensions match the hole diameter (Fig. 3e). Subsequently, the droplet moves through the plane in Fig. 3f, coating the needles of an underlying microneedle patch. A video of the droplet passing through a hole can be found in the supplementary material.

To demonstrate the process of exact and parallelizable dosage of a certain amount of liquid, weight measurements were performed using a A&DTM HR-250 AZ high precision weight scale, which provides sufficient accuracy for measuring the mass of a droplet passing through a hole in the region of $d \sim 1.3$ mm. Droplets passing through holes down to a diameter of 700 µm were observed, but results are not presented due to limitations of the measurement setup, as the expected mass of these droplets is below 1 mg, and the standard deviation of the used scale is 0.1 mg.

As long as the hole diameter is large compared to the plate height (here 100 µm), capillary forces are negligible. The moment the droplet passes the hole, the radii of curvature on top and bottom are equal (see Fig. 3e), and no forces due to a Laplacian pressure difference act on the droplet. Therefore, the droplets can pass through the hole, solely under the influence of the gravitational force.

If the dimensions of the hole are in the range of the plate height, the hole through the plate embodies a capillary. Here, droplets that enter the capillary will stick inside, as surface tension forces are much higher than the gravitational forces due to the small droplet masses. It can be expected that the proposed setup works even at smaller hole diameters, if the plate thickness can be decreased, given that the superhydrophobic coating is able to coat the inside of the holes. Otherwise, the inside of the holes would be hydrophilic, and droplets can stick inside the capillary. To this end, the setup in its current state is limited to hole diameters of about 700 µm.

The setup with a fully occupied 3×3 array of droplets resting on the holes was put above the scale and mass was tracked over time. Figure 4 shows the measured weight progression for a hole diameter of $d = 1.9$ mm at room temperature. Each jump in mass (emphasized by the red circles) represents a droplet landing on the scale. Due to

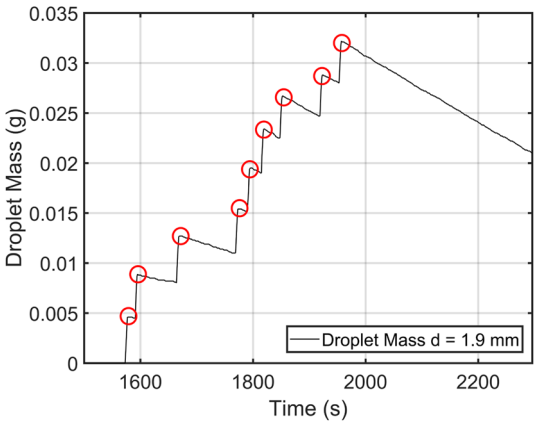

Fig. 4 Tracked mass progression for a hole diameter of $d = 1.9$ mm. The red circles indicate the moment where a droplet falls on the high precision scale through one of the nine holes

the initial dispensing stage (see Fig. 3a–c), only an approximate quantity of the liquid is placed on top of the holes of the dosage plate. As the amount of the liquid slightly varies between the dispensed droplets, bigger ones take longer to evaporate until their size matches the hole diameter, and to subsequently pass through the hole (Fig. 3f). The slow decrease of mass between the mass jumps is due to evaporation of the already dosed droplets on the scale.

Figure 5 shows the evaluation of Fig. 4 for five different hole diameters. The x-axis shows the number of the droplet which hits the weight first, second, and so forth. The y-axis shows the delivered droplet mass. Evaporation between each released droplet is eliminated by only considering the height of the jumps in Fig. 4. The standard deviation of the used scale is plotted using error bars, showing the limit of the accuracy of the scale. Figure 5 shows the repeatability of the presented concept, as the measurements with our 3×3 dosage array provide nine statistically independent events. The data show that the system can apply an equal amount of liquid every time a droplet passes through the superhydrophobic plate.

It can be seen in Fig. 3e that the droplet shape is not perfectly spherical when the droplet passes through the plane. Gravity assists in deforming the droplet overcoming surface tension forces by pulling it through the hole, slightly constricting the droplet around the perimeter of the hole. The droplet mass is, therefore, higher than that of a spherical droplet with the radius corresponding to the hole diameter.

Figure 6 shows the measured dosed mass (red crosses) and the expected mass of an ideal sphere (solid blue line) for rising hole diameters (density $\rho = 1000$ kg/m^3). The droplet profile during this transition was approximated as a modified Cassini oval, scaled for the application shown in this work. Similar

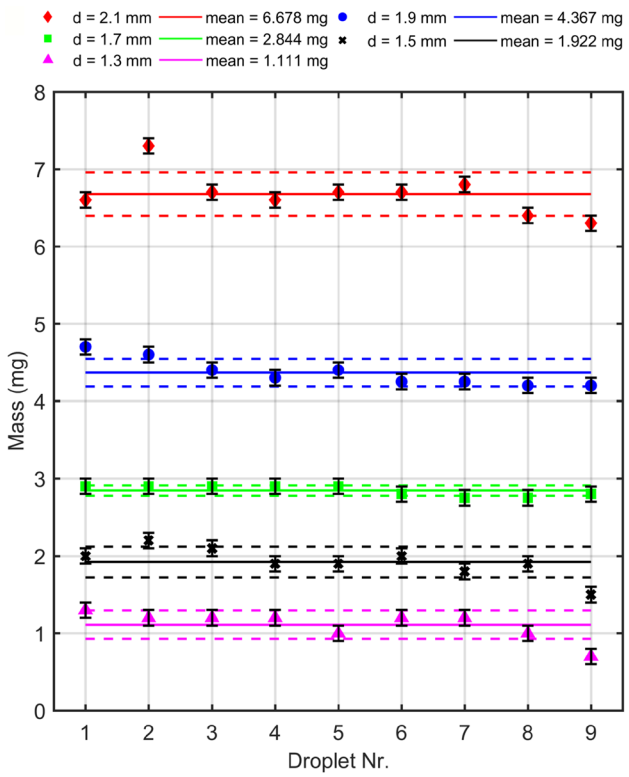

Fig. 5 Dosed droplet mass without evaporation. Points: measured data. Solid line: mean value. Dashed lines: standard deviation. The black error bars show the standard deviation of the scale

approximations were adopted by Fdida et al. (2010) and Ishikawa and Nishinari (2018). The parametric equations read

$$x(t) = \sin(t)\sqrt{a^2 \cos(2t) + \sqrt{b^4 - a^4 \sin(2t)}}$$

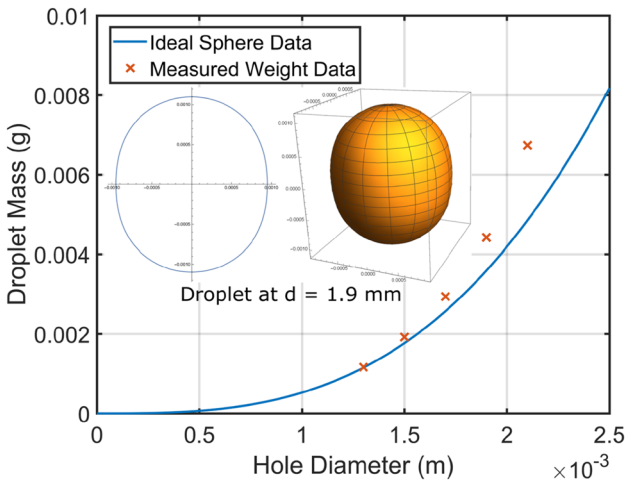

Fig. 6 Deviation of the dosed droplets from the ideal sphere. The droplet's shape during transition through the plane can be approximated as a Cassini oval (compare droplet $d = 1.9$ mm)

$$y(t) = c\cos(t)\sqrt{a^2\cos(2t) + \sqrt{b^4 - a^4\sin(2t)}} \quad (1)$$

with the parameter $t \in [0, 2\pi]$. The variables a and b are parameters describing the shape of the Cassini oval (with $a/b \in [0, 1]$), whereas c was introduced to match the specific shape of the droplet. If $a/b = 0$, the shape of the droplet matches a perfect sphere, undisturbed from gravitational forces. The more the a/b approaches unity, the more the droplet is constricted around the perimeter of the hole, accounting for the gravitational pull. The depicted Cassini oval in the inset of Fig. 6 represents the shape of a water droplet, carried through a hole with diameter $d = 1.9$ mm. The volume of the solid of revolution of the parametric curve was calculated to match the measured mean mass of 4.367 mg as the target value. The corresponding parameters are $a = 0.6677 \times 10^{-3}$, $b = 1.1612 \times 10^{-3}$ and $c = 0.82$.

Gravity influences the bigger droplets (resting on larger holes) stronger; thus, the deviation from the ideal sphere is expected to be higher. Small droplets are affected less by gravity; therefore, the spherical approximation provides better results.

In conclusion, for a droplet with diameter $d = 1.3$ mm and lower, the effects of gravity on the dosed amount are assumed to be negligible. Like noted before, droplet mass measurement for hole diameters below 1.3 mm was not possible due to experimental limitations. But according to Fig. 6, the proposed method can yield a sufficiently accurate performance in controlled dosage generation corresponding to typical microneedles with the height below 1 mm.

4 Conclusion

The present work shows a method for exact liquid dosage, simply dependent on the geometry of a superhydrophobic-coated plane. The applicability for coating microneedles with drugs is enhanced by this highly parallelizable and facile approach. Furthermore, the proposed platform could also be utilized for other applications requiring exact liquid dosage, e.g., potentially for liquid handling on microtiter plates, used for enzyme-linked immunosorbent array (ELISA) applications (Shehab 1983).

Acknowledgements Open access funding provided by Johannes Kepler University Linz. This work has been supported by the COMET-K2 "Center for Symbiotic Mechatronics" of the Linz Center of Mechatronics (LCM) funded by the Austrian federal government and the federal state of Upper Austria.

References

Alkilani A, McCrudden MT, Donnelly R (2015) Transdermal drug delivery: innovative pharmaceutical developments based on disruption of the barrier properties of the stratum corneum. Pharmaceutics 7:438–470. https://doi.org/10.3390/pharmaceutics7040438

Berthier J (2013) The physics of droplets. In: Micro-drops and digital microfluidics, chap 3.9. Elsevier, Amsterdam, pp 75–160

Chen X, Fernando GJP, Crichton ML et al (2011) Improving the reach of vaccines to low-resource regions, with a needle-free vaccine delivery device and long-term thermostabilization. J Control Release 152:349–355. https://doi.org/10.1016/j.jconrel.2011.02.026

Dash S, Garimella SV (2013) Droplet evaporation dynamics on a superhydrophobic surface with negligible hysteresis. Langmuir 29:10785–10795. https://doi.org/10.1021/la402784c

Dash S, Garimella SV (2014) Droplet evaporation on heated hydrophobic and superhydrophobic surfaces. Phys Rev E 89:042402. https://doi.org/10.1103/PhysRevE.89.042402

Fdida N, Blaisot J-B, Floch A, Dechaume D (2010) Drop-size measurement techniques applied to gasoline sprays. At Sprays 20:141–162. https://doi.org/10.1615/AtomizSpr.v20.i2.40

Gill HS, Prausnitz MR (2007) Coated microneedles for transdermal delivery. J Control Release 117:227–237. https://doi.org/10.1016/j.jconrel.2006.10.017

Haj-Ahmad R, Khan H, Arshad M et al (2015) Microneedle coating techniques for transdermal drug delivery. Pharmaceutics 7:486–502. https://doi.org/10.3390/pharmaceutics7040486

Ishikawa H, Nishinari K (2018) Modelling levitated 2-lobed droplets in rotation using Cassinian oval curves. J Fluid Mech 846:1088–1113. https://doi.org/10.1017/jfm.2018.262

Larrañeta E, McCrudden MTC, Courtenay AJ, Donnelly RF (2016) Microneedles: a new frontier in nanomedicine delivery. Pharm Res 33:1055–1073. https://doi.org/10.1007/s11095-016-1885-5

Lee H, Song C, Baik S et al (2018) Device-assisted transdermal drug delivery. Adv Drug Deliv Rev 127:35–45. https://doi.org/10.1016/j.addr.2017.08.009

Marmur A (2003) Wetting on hydrophobic rough surfaces: to be heterogeneous or not to be? Langmuir 19:8343–8348. https://doi.org/10.1021/la0344682

McGrath MG, Vrdoljak A, O'Mahony C et al (2011) Determination of parameters for successful spray coating of silicon microneedle arrays. Int J Pharm 415:140–149. https://doi.org/10.1016/j.ijpharm.2011.05.064

Patil PA (2017) Transdermal drug delivery system—a review. World J Pharm Pharm Sci 1:2049–2072. https://doi.org/10.20959/wjpps20174-9012

Prausnitz MR, Langer R (2008) Transdermal drug delivery. Nat Biotechnol 26:1261–1268. https://doi.org/10.1038/nbt.1504

Shehab ZM (1983) The enzyme-linked immunosorbent assay (ELISA). Infect Dis Newsl 2:91–92. https://doi.org/10.1016/S0278-2316(83)80010-3

Tröls A, Clara S, Jakoby B (2016) A low-cost viscosity sensor based on electrowetting on dielectrics (EWOD) forces. Sens Actuators A Phys 244:261–269. https://doi.org/10.1016/j.sna.2016.04.047

Wang S, Jiang L (2007) Definition of superhydrophobic states. Adv Mater 19:3423–3424. https://doi.org/10.1002/adma.200700934

Zang D, Li F, Geng X et al (2013) Tuning the wettability of an aluminum surface via a chemically deposited fractal dendrite structure. Eur Phys J E 36:59. https://doi.org/10.1140/epje/i2013-13059-2